

VECTOR CONTROL MODELLING OF VEHICLE TO GRID CHARGING AND DISCHARGING CONVERTER

XIAOLEI WANG, LIANG YANG, PAN YAN, WENDAO YAO AND GUANGWEN SHI

School of Electric and Information Engineering
Zhongyuan University of Technology
No. 41, Zhongyuan Road, Zhengzhou 450007, P. R. China
www.218@126.com; ylsolar@qq.com

Received May 2013; revised October 2013

ABSTRACT. *In this paper, a space vector based new control strategy and circuit topology structure of electric vehicle charging and discharging converter is proposed. The control strategy uses rotation vector of the directional three-phase active tide reversible PWM converter, and the circuit topology is two-way control DC/DC converter with double buck reversible structure. In order to improve the efficiency of vehicle to grid charging and discharging converter (V2GCDC), main circuit of the converter adopts isolation method, which is suitable for high power direct voltage battery group. The Euler-Lagrange method is used to analyze dynamic process and control method of V2GCDC. The simulation results show that the double buck reversible structure has the function of electric power flowing with two-way, the transmission power factor is 1, and the harmonic is under control within 2%.*

Keywords: V2GCDC, Vector control, Electric vehicle, Euler-Lagrange method

1. **Introduction.** V2G (Vehicle to Grid) describes a new type of grid technology, and electric vehicles are not only as users of power, but also as green energy storage units connected with power grid [1]. V2G technology is an important part of Smart Grid Technology (SGT), which can exchange energy in two ways interaction between electric vehicle and grid under controlled conditions. Application of V2G technology, electric vehicle battery can be unified arrangements in charging and discharging [2]. In accordance with charging and discharging strategy, surplus energy can be feedback to power grid. Intelligent V2GCDC usually has three-phase structure in power grid side [3]. Power can flow in positive or negative direction for the sake of using double buck chopper circuit in DC/DC converter part. Electrical energy of power grid flows to battery array in charging, and the battery arrays' energy flows to the power grid in discharging. The PWM converter/inverter circuit displays characteristics of a constant voltage source in charging, and it displays characteristics of a constant current source in discharging [4,5]. The Euler-Lagrange method is used to analyze dynamic process and control method of V2GCDC [6]. At the same time, it is comprehensively analyzed that front mathematical model of PWM rectifier/inverter and back mathematical model of the bidirectional DC/DC conversion device, to seek their common characteristics. A more versatile V2GCDC unified mathematical model is established which is based on the above two mathematical models, and can be used in simulation and control of electric vehicles in SG [7]. It can be seen from the decoupled equation of V2GCDC, rotating coordinate system orientation is not effected by differences of bidirectional DC/DC converter topology connected back of inverter which is based on vector control analysis method of PWM rectifier/inverter [8].

It is not influenced fundamentally by the source of rotation angle and changes of given parameters and feedback parameters that control strategy of overall V2GCDC [9].

Using concept of PWM rectifier/inverter for different types of DC/DC converter, after decoupling operator, PWM rectifier/inverter of V2GCDC has similar equations with various types of voltage equations with DC/DC transform [10]. Therefore, the coordinate oriented vector control can be used in control strategy. V2GCDC is a complex hybrid AC-DC power control system, which has certain theoretical and practical significance based on kinetic energy balance of the Euler-Lagrange equation to analyze process of charging and discharging transient [11,12]. Therefore, in this paper, a space vector based new control strategy and circuit topology structure of electric vehicle charging and discharging converter are proposed.

The outline of the paper is given as follows. Basic constraints of V2GCDC is described in Section 2. The Euler-Lagrange Equation in application of electricity control system and transformation device is presented in Section 3. The Euler-Lagrange Equation in application of V2GCDC is discussed in Section 4. The simulation results are given in Section 5, and Section 6 is the conclusion.

2. Basic Constraints of V2GCDC.

2.1. Typical structure of V2GCDC. The typical structure of V2GCDC is shown in Figure 1. Voltage of power grid is equivalent to three-phase symmetric alternating voltage source, alternating voltage is u_x ($x = A, B, C$), frequency of power grid is f , and radian frequency of power grid is ω . The power grid is connected to switch elements of IGBT through a group of inductance components, current of inductance components are i_A, i_B, i_C . The type of inverter is a three-phase bridge, which includes six switch elements (T_1 - T_6) and six freewheel diodes (D_1 - D_6).

2.2. Basic switch constraints of V2GCDC. Every branch of PWM rectifier/inverter has a basic switch constraint, that is, the branch T_1 and T_4 complementary, T_3 and T_6 complementary, T_5 and T_2 complementary, T_7 and T_8 complementary. The switch state function of every branch is decided by the above half bridge's switch condition or below half bridge's switch condition, freewheel diode only influence to freewheeling loop. In the following we will make such a hypothesis that the DC bus voltage between P and N is V_{dc} , the potential of P is V_{dc} , the potential of N is 0, and voltage of all capacitors is in balance states. We can get the output voltage of every phase through the switch condition of every branch, which is shown in Table 1. The number 1 represents that the switch is

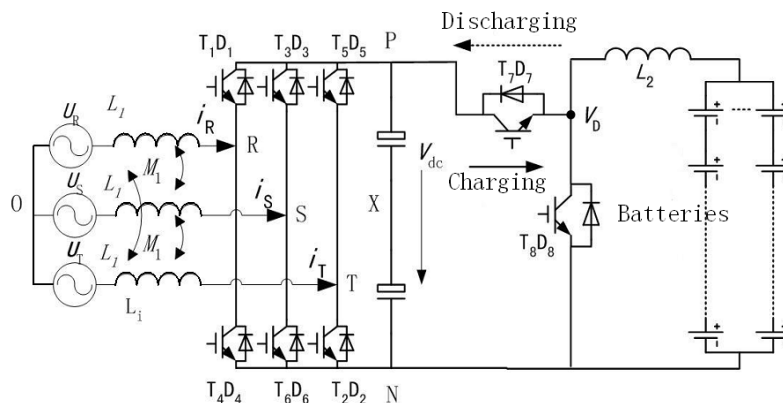


FIGURE 1. The typical structure of V2GCDC

TABLE 1. Relationship between three-phase switch function and voltage

S_C	S_B	S_A	V_{AN}	V_{BN}	V_{CN}	V_{AB}	V_{BC}	V_{CA}
0	0	0	0	0	0	0	0	0
0	0	1	$2V_{DC}/3$	$-V_{DC}/3$	$-V_{DC}/3$	V_{DC}		$-V_{DC}$
0	1	0	$-V_{DC}/3$	$2V_{DC}/3$	$-V_{DC}/3$	$-V_{DC}$	V_{DC}	
0	1	1	$V_{DC}/3$	$V_{DC}/3$	$-2V_{DC}/3$		V_{DC}	$-V_{DC}$
1	0	0	$-V_{DC}/3$	$-V_{DC}/3$	$2V_{DC}/3$		$-V_{DC}$	V_{DC}
1	0	1	$V_{DC}/3$	$-2V_{DC}/3$	$V_{DC}/3$	V_{DC}	$-V_{DC}$	
1	1	0	$-2V_{DC}/3$	$V_{DC}/3$	$V_{DC}/3$	$-V_{DC}$		V_{DC}
1	1	1	0	0	0	0	0	0

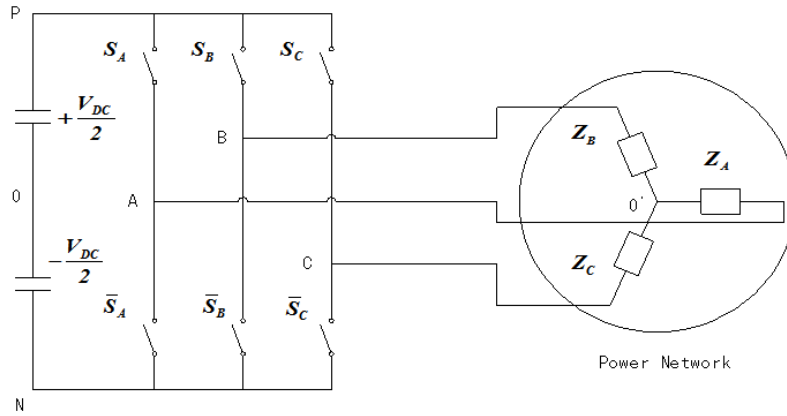


FIGURE 2. The typical V2G structure of V2GCDC

on and the number 0 represents that the switch is off. The letter j represents the set of all phases of PWM rectifier/inverter and DC/DC converter, which is shown in the following. $j \in (A, B, C, D)$, S_j is the switch function of every switch, and $S_j = (1, 0)$.

The simplified main circuit topology structure of three-phase bridge inverter is shown in Figure 2, and the switch elements such as IGBT, IPM or other elements in the same place have the same switch function. We can get the line voltage and phase voltage with different compound modes through the given value of DC voltage, which is shown in Table 1.

2.3. The voltage constraints equations of PWM rectifier/inverter in the side of power grid. The voltage constraints equations of PWM rectifier/inverter in the side of power grid relate with connection type of three-phase winding, when the connection type of three-phase winding is Y , and the equation can be described as,

$$Q_{j'} = u_{j'} = (u_{j'N} - u_{NO'j'}) \quad j' \in (A, B, C) \quad (1)$$

where $u_{j'N}$ represents the potential of N in the three-phase winding, and $u_{NO'j'}$ is the poor between the potential of N and the potential of $O'j'$. Therefore, we can obtain voltage constraints equations based on axiom of Kirchhoff's Voltage Laws (KVL) and Kirchhoff's Current Laws (KCL),

$$U_{NO'j'} = -\frac{1}{3}(U_{AN} + U_{BN} + U_{CN}) \quad (2)$$

Moreover, the voltage of PWM rectifier/inverter's every phase can be obtained,

$$U_{j'N} = S_{j'}V_{DC} \quad (3)$$

3. The Euler-Lagrange Equation in Application of Electricity Control System and Transformation Device. The Euler-Lagrange equation of electricity control system and transformation device is described as,

$$\frac{d}{dt} \left(\frac{\partial L}{\partial i_j} \right) - \frac{\partial L}{\partial q_j} + \frac{\partial F}{\partial i_j} = Q_j \quad (j = A, B, C, L) \quad (4)$$

where, the letter of L represents Lagrange equation, which equals the poor between Kinetic energy (T) and potential energy (V). The letter of q_j is generalized coordinate, and q_A , q_B , q_C and q_L of the electrical system are the generalized coordinates. The letter of i_j is generalized velocity, and i_A , i_B , i_C and i_L of the electrical system are the generalized velocities. The letter of F represents dissipation function, which is the loss energy of resistance, and,

$$F = \frac{1}{2} R_A i_A^2 + R_B i_B^2 + R_C i_C^2 + R_{L2} i_D^2 + R_S i_D^2 \quad (5)$$

The letter of R_s represents loss factors, which are R_A , R_B , R_C and R_L . The letters ψ_A , ψ_B , ψ_C and ψ_D of flux linkage represent generalized momentum.

According to the above relationship and Figure 2, the mathematical model of PWM rectifier/inverter can be obtained. There is generalized potential energy for the sake of the existence of capacitor. Therefore, the Lagrange equation is established, which is shown in the following,

$$L = T' - V \quad (6)$$

The generalized potential energy is shown in the following,

$$V = \frac{1}{2} \frac{q^2}{C} \quad (7)$$

where, the letter q is the Charge of DC capacitor (C), which is shown in the following that relationship between the Charge (q_x) of inductance component and the Charge (q) of C ,

$$q_x = \frac{q}{S'_x} \quad x = A, B, C, D \quad (8)$$

where the letter S'_x is the switch function.

$$q_L = q \quad (9)$$

The load is a resistive load in usual conditions, so there is no inductor. It is got that the generalized kinetic energy equation of Figure 2, is

$$T' = W'_c(i_A, i_B, i_C) \quad (10)$$

Then, the generalized force equation of voltage can be obtained based on Equations (4)-(10), namely,

$$\frac{d}{dt} \left[\frac{\partial W'_c(i_A, i_B, i_C, i_D)}{\partial i_j} \right] + R_{j'} i_{j'} - \frac{\partial V}{\partial q_{j'}} = u_{j'} \quad (11)$$

In Equation (11), the relationship between potential energy and generalized displacement charge can be described,

$$\frac{\partial V}{\partial q_x} = -\frac{\partial \left(\frac{1}{2} \frac{q^2}{C} \right)}{\partial q_x} = -S'_x \frac{\partial \left(\frac{1}{2} \frac{q^2}{C} \right)}{\partial q} = -S'_x \frac{q}{C} = -S'_x V_{dc}, \quad x = A, B, C, D \quad (12)$$

The negative sign represents reducing trend of generalized velocity. Then the voltage switch functions can be obtained based on the above relationship,

$$\begin{aligned} S'_A &= \frac{2}{3} S_A - \frac{1}{3} S_B - \frac{1}{3} S_C \\ S'_B &= \frac{2}{3} S_B - \frac{1}{3} S_C - \frac{1}{3} S_A \end{aligned}$$

$$S'_C = \frac{2}{3}S_C - \frac{1}{3}S_A - \frac{1}{3}S_B \quad (13)$$

where S_x equals 1 which represents that the above bridge is on, and it equals 0 which represents that the above bridge is off ($x = A, B, C$).

Therefore, the generalized force potential energy of the load (Z_L) can be shown in the following,

$$\frac{\partial V}{\partial q_L} = \frac{\partial \left(\frac{1}{2} \frac{q^2}{C} \right)}{\partial q_L} = \frac{\partial \left(\frac{1}{2} \frac{q^2}{C} \right)}{\partial q} = \frac{q}{C} = V_{dc} = u'_L \quad (14)$$

Because the magnetic altogether energy different current is flux linkage, the flux linkage function of PWM rectifier/inverter can be obtained,

$$\frac{\partial W'_c(i_A, i_B, i_C, i_D)}{\partial i_{j'}} = \psi_{j'}(i_A, i_B, i_C, i_D), \quad j' \in (A, B, C, D) \quad (15)$$

4. The Euler-Lagrange Equation in Application of V2GCDC.

4.1. **The flux linkage function of PWM rectifier/inverter.** According to Equations (11)-(15), the equations of PWM rectifier/inverter and two-way control DC/DC converter can be obtained,

$$\frac{\partial \psi_A}{\partial i_A} \frac{di_A}{dt} + \frac{\partial \psi_A}{\partial i_B} \frac{di_B}{dt} + \frac{\partial \psi_A}{\partial i_C} \frac{di_C}{dt} + \frac{\partial \psi_A}{\partial i_D} \frac{di_D}{dt} + S'_A V_{dc} + R_A i_A = u_A \quad (16)$$

$$\frac{\partial \psi_B}{\partial i_A} \frac{di_A}{dt} + \frac{\partial \psi_B}{\partial i_B} \frac{di_B}{dt} + \frac{\partial \psi_B}{\partial i_C} \frac{di_C}{dt} + \frac{\partial \psi_B}{\partial i_D} \frac{di_D}{dt} + S'_B V_{dc} + R_B i_B = u_B \quad (17)$$

$$\frac{\partial \psi_C}{\partial i_A} \frac{di_A}{dt} + \frac{\partial \psi_C}{\partial i_B} \frac{di_B}{dt} + \frac{\partial \psi_C}{\partial i_C} \frac{di_C}{dt} + \frac{\partial \psi_C}{\partial i_D} \frac{di_D}{dt} + S'_C V_{dc} + R_C i_C = u_C \quad (18)$$

$$\frac{\partial \psi_D}{\partial i_A} \frac{di_A}{dt} + \frac{\partial \psi_D}{\partial i_B} \frac{di_B}{dt} + \frac{\partial \psi_D}{\partial i_C} \frac{di_C}{dt} + \frac{\partial \psi_D}{\partial i_D} \frac{di_D}{dt} + S'_D V_{dc} + R_D i_D = u_D \quad (19)$$

$$u_D = E_0 - i_D R_S \quad (20)$$

Then, the current constraint equation of the capacitor loop based on the KCL can be obtained,

$$C \frac{dV_{dc}}{dt} = (S_A i_A + S_B i_B + S_C i_C) - S_D i_D \quad (21)$$

And, the voltage matrix equation of PWM rectifier/inverter can also be obtained,

$$\mathbf{U} = \mathbf{R} \cdot \mathbf{I} + p\boldsymbol{\psi} \quad (22)$$

where $p = \frac{d}{dt}$ is the differential operator. Equation (22) also can be written in such style,

$$\mathbf{U} = \begin{bmatrix} u_A - \left(\frac{2}{3}S_A - \frac{1}{3}S_B - \frac{1}{3}S_C \right) V_{dc} \\ u_B - \left(\frac{2}{3}S_B - \frac{1}{3}S_C - \frac{1}{3}S_A \right) V_{dc} \\ u_C - \left(\frac{2}{3}S_C - \frac{1}{3}S_A - \frac{1}{3}S_B \right) V_{dc} \\ E_0 - S_D V_{dc} \end{bmatrix} \quad (23)$$

$$\mathbf{I} = [i_A \quad i_B \quad i_C \quad i_D]^T \quad (24)$$

$$\mathbf{R} = \text{diag} [R_A \quad R_B \quad R_C \quad R_D] \quad (25)$$

$$\boldsymbol{\psi} = [\psi_A \quad \psi_B \quad \psi_C \quad \psi_D]^T \quad (26)$$

According to the above equation, the conventional voltage equation is obtained,

$$\mathbf{U} = \mathbf{I} \cdot \mathbf{R} + \mathbf{L} \cdot p\mathbf{I} \quad (27)$$

And, the matrix of inductor is shown in the following,

$$\mathbf{L} = \begin{bmatrix} \frac{\partial \psi_A}{\partial i_A} & \frac{\partial \psi_A}{\partial i_B} & \frac{\partial \psi_A}{\partial i_C} & 0 \\ \frac{\partial \psi_B}{\partial i_A} & \frac{\partial \psi_B}{\partial i_B} & \frac{\partial \psi_B}{\partial i_C} & 0 \\ \frac{\partial \psi_C}{\partial i_A} & \frac{\partial \psi_C}{\partial i_B} & \frac{\partial \psi_C}{\partial i_C} & 0 \\ 0 & 0 & 0 & \frac{\partial \psi_D}{\partial i_D} \end{bmatrix} \quad (28)$$

If the inductors are linear elements, we can get the following equation,

$$\boldsymbol{\psi} = \mathbf{L} \cdot \mathbf{I} \quad (29)$$

Therefore, Equation (22) can be changed into the following equation,

$$\begin{bmatrix} S'_A V_{dc} \\ S'_B V_{dc} \\ S'_C V_{dc} \\ S'_D V_{dc} \end{bmatrix} = \begin{bmatrix} u_{AS} \\ u_{BS} \\ u_{CS} \\ u_D \end{bmatrix} = - \begin{bmatrix} R_A & & & \\ & R_B & & \\ & & R_C & \\ & & & R_{L2} + R_S \end{bmatrix} \begin{bmatrix} i_A \\ i_B \\ i_C \\ i_D \end{bmatrix} - p \begin{bmatrix} \psi_A \\ \psi_B \\ \psi_C \\ \psi_D \end{bmatrix} + \begin{bmatrix} u_A \\ u_B \\ u_C \\ E_0 \end{bmatrix} \quad (30)$$

New voltage matrices are defined in Matrix (30), which are shown in the following,

$$\mathbf{U}_s = [u_{AS} \quad u_{BS} \quad u_{CS} \quad u_D]^T \quad (31)$$

$$\mathbf{U}_e = [u_A \quad u_B \quad u_C \quad E_0]^T \quad (32)$$

In linear conditions, the matrix of inductor is defined by,

$$L = \frac{\partial \psi_A}{\partial i_A} = \frac{\partial \psi_B}{\partial i_B} = \frac{\partial \psi_C}{\partial i_C} \quad (33)$$

$$-M = \frac{\partial \psi_x}{\partial i_y}, \quad x = A, B, C; \quad y = A, B, C; \quad x \neq y \quad (34)$$

Matrix (29) of flux linkage also can be written in the following style,

$$\begin{bmatrix} \psi_A \\ \psi_B \\ \psi_C \\ \psi_D \end{bmatrix} = \begin{bmatrix} L & -M & -M & 0 \\ -M & L & -M & 0 \\ -M & -M & L & 0 \\ 0 & 0 & 0 & L_2 \end{bmatrix} \begin{bmatrix} i_A \\ i_B \\ i_C \\ i_D \end{bmatrix} = \mathbf{L}_{ABCD} \mathbf{I}_{ABCD} \quad (35)$$

And, the voltage Equation (30) also can be written in such style,

$$\mathbf{U}_s = -\mathbf{R}\mathbf{I} - p\boldsymbol{\psi} + \mathbf{U}_e \quad (36)$$

4.2. Coordinate transformation of PWM rectifier/inverter's electrical energy and converter device. The power transformation network of PWM rectifier/inverter uses synchronous d - q -0 coordinate system. The power transformation scheme is shown in Figure 3.

In Figure 3, the d - q coordinate system is rotating with radian frequency (ω) of power grid, and letter θ is rotation angle of coordinate system. The direction of d axis is decided by direction of synthetic voltage vector. Transformation matrix can be shown,

$$\mathbf{K}(\theta) = \frac{2}{3} \begin{bmatrix} \sin \theta & \sin(\theta - \frac{2\pi}{3}) & \sin(\theta + \frac{2\pi}{3}) & 1 \\ \cos \theta & \cos(\theta - \frac{2\pi}{3}) & \cos(\theta + \frac{2\pi}{3}) & 1 \end{bmatrix} \quad (37)$$

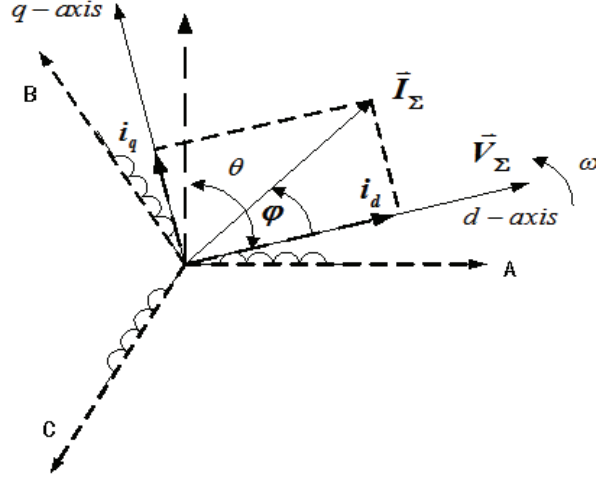


FIGURE 3. The power transformation scheme

Inverse transformation matrix is described as,

$$\mathbf{K}^{-1}(\theta) = \mathbf{K}^T(\theta) = \begin{bmatrix} \sin \theta & \cos \theta \\ \sin \left(\theta - \frac{2\pi}{3} \right) & \cos \left(\theta - \frac{2\pi}{3} \right) \\ \sin \left(\theta + \frac{2\pi}{3} \right) & \cos \left(\theta + \frac{2\pi}{3} \right) \\ 1 & 1 \end{bmatrix} \quad (38)$$

Therefore, according to Equations (24)-(27), the new vector matrix can be obtained,

$$\mathbf{U}_s = \mathbf{K}^{-1}(\theta)\mathbf{U}_{dqs} \quad (39)$$

$$\mathbf{U}_e = \mathbf{K}^{-1}(\theta)\mathbf{U}_{dqe} \quad (40)$$

$$\mathbf{I} = \mathbf{K}^{-1}(\theta)\mathbf{I}_{dq} \quad (41)$$

$$\boldsymbol{\psi} = \mathbf{K}^{-1}(\theta)\boldsymbol{\psi}_{dq} \quad (42)$$

Equation (36) also can be changed into the following style,

$$\mathbf{K}(\theta)\mathbf{K}^{-1}(\theta)\mathbf{U}_{dqs} = -\mathbf{K}(\theta)\mathbf{R}\mathbf{K}^{-1}(\theta)\mathbf{I}_{dq} - \mathbf{K}(\theta)p[\mathbf{K}^{-1}(\theta)\boldsymbol{\psi}_{dq}] + \mathbf{K}(\theta)\mathbf{K}^{-1}(\theta)\mathbf{U}_{dqe} \quad (43)$$

In Equation (43), the voltage matrix of power grid and battery in d - q coordinate system can be described,

$$\mathbf{U}_{dqe} = \mathbf{K}(\theta)\mathbf{U}_e = [u_{de} \quad u_{qe} \quad E_0]^T \quad (44)$$

And the switch voltage matrix of inverter in d - q coordinate system is described,

$$\mathbf{U}_{dqs} = \mathbf{K}(\theta)\mathbf{U}_s = [u_{ds} \quad u_{qs} \quad u_D]^T \quad (45)$$

Current matrix is described in d - q coordinate system,

$$\mathbf{I}_{dq} = \mathbf{K}(\theta)\mathbf{I} = [i_d \quad i_q \quad i_D]^T \quad (46)$$

Flux linkage matrix is shown,

$$\boldsymbol{\psi}_{dq} = \mathbf{K}(\theta)\boldsymbol{\psi} = [\psi_d \quad \psi_q \quad \psi_D]^T \quad (47)$$

And the resistance matrix is shown,

$$\mathbf{R}_{dq} = \mathbf{K}(\theta)\mathbf{R}\mathbf{K}^{-1}(\theta) = \text{diag} [R_d \quad R_q \quad R_{L2} + R_S] \quad (48)$$

4.3. Coordinate transformation voltage equations of PWM rectifier/inverter and bidirectional DC/DC converter. Voltage equations have the following styles in d - q coordinate system, first,

$$\mathbf{U}_{dqs} = -\mathbf{R}_{dq}\mathbf{I}_{dq} - \mathbf{K}(\theta)p[\mathbf{K}^{-1}(\theta)\boldsymbol{\psi}_{dq}] + \mathbf{U}_{dqe} \quad (49)$$

And, Equation (49) also can be written as,

$$\mathbf{U}_{dqs} = -\mathbf{R}_{dq}\mathbf{I}_{dq} - \mathbf{K}(\theta)p[\mathbf{K}^{-1}(\theta)]\boldsymbol{\psi}_{dq} - \mathbf{K}(\theta)[\mathbf{K}^{-1}(\theta)]p\boldsymbol{\psi}_{dq} + \mathbf{U}_{dqe} \quad (50)$$

In Equation (50), the flux linkage equation can be written in the following style,

$$\boldsymbol{\psi}_{dq} = \mathbf{K}(\theta)L_{ABCD}\mathbf{K}^T(\theta)\mathbf{I}_{dq} = \mathbf{L}_{dq}\mathbf{I}_{dq} \quad (51)$$

Therefore, we can obtain the following equation based on the differential chain law,

$$\mathbf{K}(\theta)p[\mathbf{K}^{-1}(\theta)] = \frac{\partial\mathbf{K}^{-1}(\theta)}{\partial\theta}\frac{d\theta}{dt} = \omega \begin{bmatrix} 0 & -1 \\ 1 & 0 \end{bmatrix} \quad (52)$$

Therefore, Equation (44) can be changed into the following equation,

$$\begin{bmatrix} u_{ds} \\ u_{qs} \\ u_D \end{bmatrix} = - \begin{bmatrix} R_d & & \\ & R_q & \\ & & R_{L2} + R_S \end{bmatrix} \begin{bmatrix} i_d \\ i_q \\ i_D \end{bmatrix} - \begin{bmatrix} L_d & & \\ & L_q & \\ & & L_2 \end{bmatrix} p \begin{bmatrix} i_d \\ i_q \\ i_D \end{bmatrix} - \begin{bmatrix} 0 & -\omega L_q & 0 \\ \omega L_d & 0 & 0 \\ 0 & 0 & 0 \end{bmatrix} \begin{bmatrix} i_d \\ i_q \\ i_D \end{bmatrix} + \begin{bmatrix} u_{de} \\ u_{qe} \\ E_0 \end{bmatrix} \quad (53)$$

And Equation (53) can also be changed into voltage equations, which are shown by the following equations,

$$u_{ds} = -R_d i_d - L_d p i_d + \omega L_q i_q + u_{de} \quad (54)$$

$$u_{qs} = -R_q i_q - L_q p i_q - \omega L_d i_d + u_{qe} \quad (55)$$

$$u_D = -(R_{L2} + R_S) i_D - L_2 p i_D + E_0 \quad (56)$$

4.4. The switch equation of PWM rectifier/inverter's electrical energy and converter device. According to Equations (39) and (45), we can obtain the following equation,

$$\mathbf{U}_s = \mathbf{K}^{-1}(\theta)\mathbf{U}_{dqs} = \mathbf{S}_{ABCD}^U V_{DC} \quad (57)$$

Define

$$\mathbf{S}_{dq}^U = \mathbf{K}(\theta)\mathbf{S}_{ABCD}^U = [S_d \ S_q \ S_D]^T \quad (58)$$

where S_d is switch equation of d axis and S_q is switch equation of q axis. Then, we can get the switch equation based on Equation (37).

$$S_d = \frac{2}{3} \left[S_A \sin \theta + S_B \sin \left(\theta - \frac{2\pi}{3} \right) + S_C \sin \left(\theta + \frac{2\pi}{3} \right) \right] \quad (59)$$

$$S_q = \frac{2}{3} \left[S_A \cos \theta + S_B \cos \left(\theta - \frac{2\pi}{3} \right) + S_C \cos \left(\theta + \frac{2\pi}{3} \right) \right] \quad (60)$$

Therefore, the switch equation of PWM rectifier/inverter's electrical energy and converter device can be obtained based on Equation (21) and the above equations,

$$\begin{aligned} S_A i_A + S_B i_B + S_C i_C + S_D i_D &= [S_A \ S_B \ S_C \ S_D] \begin{bmatrix} i_A \\ i_B \\ i_C \\ i_D \end{bmatrix} \\ &= [S_A \ S_B \ S_C \ S_D] \mathbf{K}^T(\theta)\mathbf{I}_{dq} = \mathbf{S}_{dq}^I \mathbf{I}_{dq} \end{aligned} \quad (61)$$

5. **Simulation of V2GCDC.** A simulation model of V2GCDC is established, and is shown in Figure 4, and the simulation results of charging are shown in Figures 5 and 6. According to Figures 5 and 6, we can find that the controlled voltage is consistent with the given voltage value. And a phase of voltage and current at the side of power grid is no difference, so the transmission power factor of the converter is 1. The simulation result of the phase current of harmonic analysis with charging is shown in Figure 7, where, we can find that the total current harmonic distortion (TCHD) rate is 0.07%.

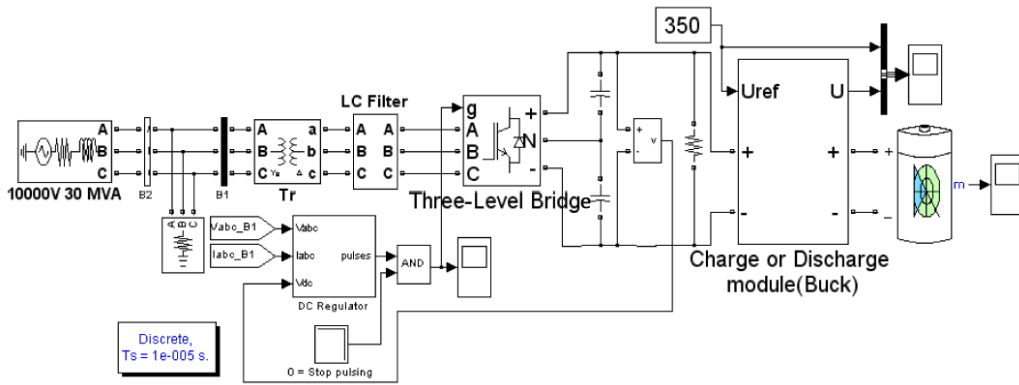


FIGURE 4. Simulation of the V2GCDC

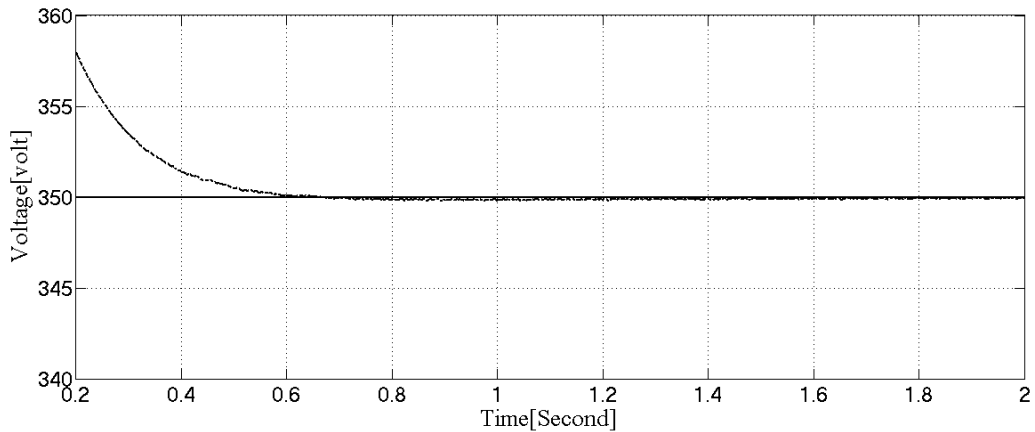


FIGURE 5. Simulation result of charging

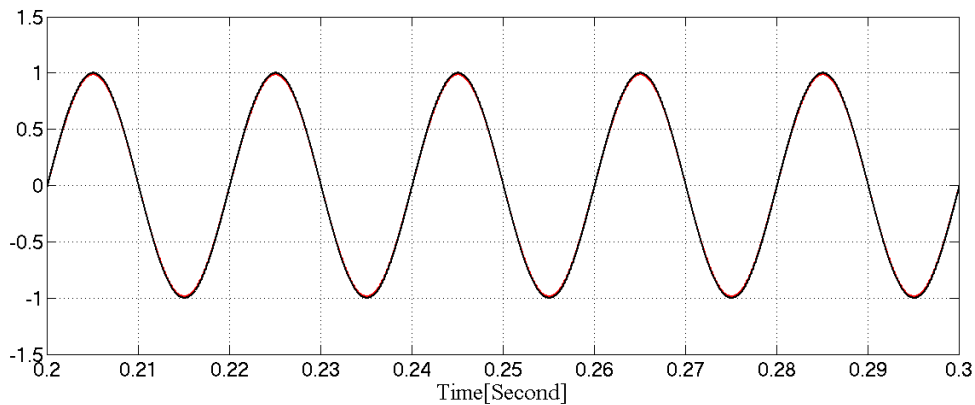


FIGURE 6. Phase of voltage and current at the side of power grid in charging

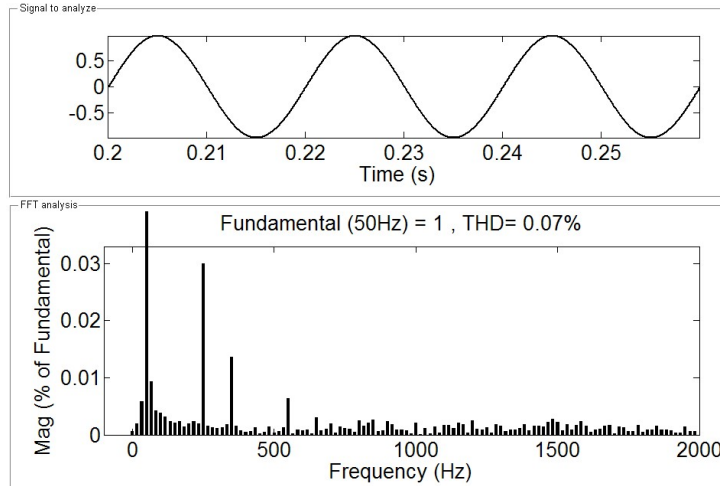


FIGURE 7. A phase's current of harmonic analysis in charging

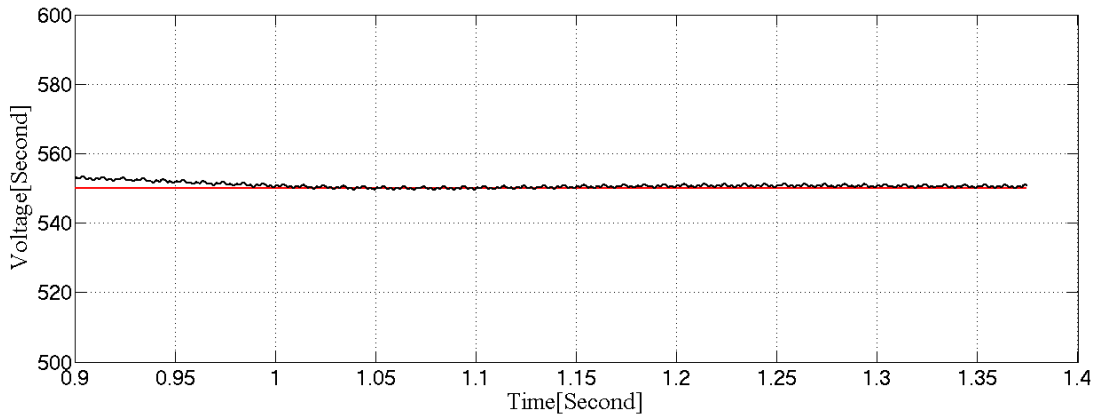


FIGURE 8. Simulation result of discharging

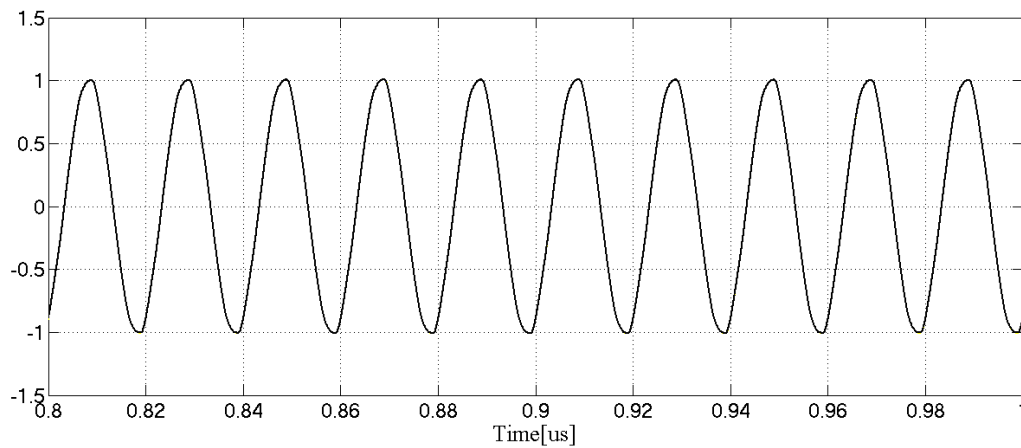


FIGURE 9. Phase of voltage and current at the side of power grid in discharging

Simulation results of discharging are shown in Figures 8 and 9. From Figures 8 and 9, we can find that controlled voltage is consistent with the given voltage value. And the phase of voltage and current at the side of power grid is no difference, so the transmission power factor of the V2GCDC is 1 in discharging. The simulation result of a phase's

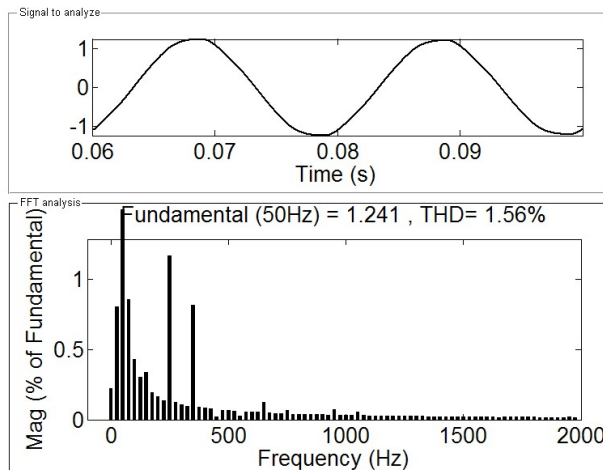


FIGURE 10. A phase's current of harmonic analysis in discharging

current of harmonic analysis with discharging is shown in Figure 10, where we can find that the total current harmonic distortion (TCHD) rate is 1.56%.

6. Conclusion. A new type of main circuit topology and control strategy about V2G-CDC is investigated, which is based on three-phase active reversible PWM rectifier using space rotation vector method. The controlled Dual-Buck of charging and discharging topology in Dual-DC/DC converter is studied. In order to improve efficiency of V2GCDC, its main circuit is non-isolated group mode, which suits for high DC voltage battery pack. PWM rectifier uses three-phase structure in power grid side, and the section of DC/DC converter uses Dual-Buck reversible charging and discharging converter, so DC energy can flow in two directions. With scheduling instructions of smart grid, the battery group can be charged from power grid, and DC energy of the battery group can also be discharged to power grid through grid-connected inverter. Grid-connected PWM rectifier/inverter has two characteristics, one is constant voltage source in rectifier charging, and the other is constant current source in discharging to power grid. PWM rectifier uses rotation oriented method of synthesized voltage vector, which achieves unity power factor to improve the input current waveform. PWM rectifier/inverter topology and control strategy can be used in two-way flow of electricity, thereby controlling in two-way trend of bilateral AC and DC V2G needing. The Euler-Lagrange method is used to analyze the dynamic process and control strategy of V2GCDC. Meanwhile, it analyzed the front PWM converter/inverter mathematics model and the two-way DC/DC converter to find their same characteristics. And it is established a uniform mathematics model of V2GCDC, which can be used in simulation and control process.

REFERENCES

- [1] T. Sousa, H. Morais, Z. Vale, P. Faria and J. Soares, Intelligent energy resource management considering vehicle-to-grid: A simulated annealing approach, *IEEE Trans. Smart Grid*, vol.3, no.1, pp.535-542, 2012.
- [2] M. Yilmaz and P. Krein, Review of the impact of vehicle-to-grid technologies on distribution systems and utility interfaces, *IEEE Trans. Power Electronics*, vol.28, no.12, pp.5673-5689, 2013.
- [3] B. Sovacool and R. Hirsch, Beyond batteries: An examination of the benefits and barriers to plug-in hybrid electric vehicles (PHEVs) and a vehicle-to-grid (V2G) transition, *Energy Policy*, vol.37, no.3, pp.1095-1103, 2009.
- [4] S. Tung, D. Hopkins and C. Mosling, Extension of battery life via charge equalization, *IEEE Trans. Ind. Electron.*, vol.40, no.1, pp.96-104, 1993.

- [5] C. Liu and S. Zhu, Design of a non-dissipative bidirectional charge/discharge equalization module for series-connected battery strings, *Control and Automation*, vol.35, no.7, pp.251-253, 2006.
- [6] D. Basic, F. Malrait and P. Rouchon, Euler-Lagrange models with complex currents of three-phase electrical machines and observability issues, *IEEE Trans. Automatic Control*, vol.55, no.1, pp.212-217, 2010.
- [7] L. Lei, X. Gai, S. Yang and L. Xi, Three-port bidirectional equalization circuit for EV power battery strings, *Power Electronics*, vol.41, no.11, pp.56-58, 2009.
- [8] F. Wang and B. Li, Equalization control strategy of batteries on clark converter, *Automobile Science and Technology*, vol.37, no.3, pp.36-39, 2008.
- [9] U. Chukwu and S. Mahajan, V2G electric power capacity estimation and ancillary service market evaluation, *Power and Energy Society General Meeting*, vol.28, no.8, pp.1-8, 2011.
- [10] S. Han, S. Han and K. Sezaki, Estimation of achievable power capacity from plug-in electric vehicles for V2G frequency regulation: Case studies for market participation, *IEEE Trans. Smart Grid*, vol.2, no.4, pp.632-641, 2011.
- [11] Y. Tang, H. Zhu, B. Song, J. S. Lai and C. Chen, EMI experimental comparison of PWM inverter between hard and soft-switching techniques, *Power Electron. Transport*, vol.37, no.5, pp.71-77, 1998.
- [12] B. Schweighofer, K. M. Raab and G. Brasseur, Modeling of high power automotive batteries by the use of an automated test system, *IEEE Trans. Instrum Mea.*, vol.52, no.4, pp.1087-1091, 2003.